Motion of the Front between Thick and Thin Film: Hydrodynamic Theory and Experiment with Vertical Foam Films

Simeon D. Stoyanov,[†] Vesselin N. Paunov,*[,†] Elka S. Basheva,[†] Ivan B. Ivanov,[†] Ammanuel Mehreteab,[‡] and Guy Broze[§]

Laboratory of Thermodynamics and Physico-chemical Hydrodynamics, Faculty of Chemistry, University of Sofia, 1126 Sofia, Bulgaria, Colgate-Palmolive R & D, Inc., Avenue Du Parc Industriel, B-4041 Milmort, Belgium, and Colgate-Palmolive Co., Technology Center, 909 River Road, Piscataway, New Jersey 08854-5596

Received August 13, 1996. In Final Form: November 7, 1996[⊗]

The motion of the front between thick and thin foam film formed in a vertical frame is studied both experimentally and theoretically. In the experiments we used sodium dodecyl sulfate solutions with added NaCl. The rate of motion of the front turns out to be *constant* for a given electrolyte concentration. Other important quantities that are measured are the thickness of the black film and the jump of the film tension, when the front reaches the bottom meniscus. The rate of the front turns out to be proportional to the jump of the film tension irrespective of the amount of added electrolyte. The theoretical model we developed allows quantitative interpretation of the experimental data. It is demonstrated that the motion of the front "thick−thin" film is accompanied with the formation of microscopic steady capillary waves in the transition zone. We show that the energy dissipation in the film is concentrated mainly into the latter part of the transition zone. The study can be helpful for the understanding of the mechanism of the foam films drainage as related to the stability of foams.

1. Introduction

Foams are of great importance in many technological processes and applications, and their properties are subject of intensive studies from both practical and scientific points of view. The properties and stability of foams are closely related to the behavior of the foam structural elements: liquid films and Gibbs−Plateau borders (GPB). The rate of foam drainage is determined from both the thinning of the foam films and the drainage of liquid from GPB. In this study we investigate both experimentally and theoretically the drainage of a single vertical film as a model system for the drainage of the thin films in the foams.

Yamanaka[1,2] studied experimentally the drainage of macroscopic single foam films confined in a vertical glass frame. The foam films were formed by drawing the frame up from a solution containing surfactant and electrolyte. Two stages of thinning of such a film can be distinguished. During the first stage the thick foam film is draining under the combined action of capillary suction of the bottom meniscus and gravity. This stage ends with the formation of a stripe of thin black film at the top of the frame. The second stage is related to the motion of the front between the black (thin) and the thick foam film downward until it reaches the capillary meniscus. In this respect the front motion resembles very much the expansion of black spots in circular films formed in the Scheludko cell, reported by other authors.[3,4]

Few important characteristics of the vertical film drainage are liable to experimental measurement. One of them is the velocity of the front between the thin and thick foam film, which is usually measured by recording of the process of film drainage with a CCD camera and consequent image analysis. The front is moving with constant velocity, v, for a given type and concentration of surfactant and electrolyte. Another important measurable quantity is the thickness of the black film, which is determined interferometrically. We use a very sensitive tensiometer to detect the jump of the film tension, $\Delta\gamma$, which occurs when the front of the thin (black) film reaches the bottom meniscus. The values of this additional tension, $\Delta\gamma$, and of the front rate, v, depend strongly on the type of surfactant and on the added electrolytes. However, the black film expansion rate, v, turns out to be proportional to $\Delta\gamma$ irrespective of the kind and the amount of added electrolytes as well as of the type of surfactant.[1,2]

These experimental findings call for development of a theoretical model explaining the mechanism of the foam film drainage and quantitatively describing the experimental data for the driving force and the rate of the front motion. The available theoretical approaches concern the case of expansion of *circular black spots* in horizontal films (for a detailed review see, e.g., ref 5). Traykov *et al.*[6] have assumed that the energy dissipation during the circular black spot expansion is concentrated in the thicker film, while Dimitrov[7,8] has considered the other extreme case when the energy dissipation occurs only in the transition zone, while the liquid in the thicker film is being quiescent. As pointed out in ref 5, common disadvantages of both approaches are the assumed shape of the interface and the omission of the surface forces that interplay with the viscous friction and capillary pressure in determining of the shape of the transition zone.

The aim of the present study is to describe theoretically the motion of the front between thin and thick vertical

* Author for correspondence: e-mail, vp@ltph.chem.uni-sofia.bg, veselin.paunov@ltph.cit.bg.
[†] University of Sofia.
[‡] Colgate-Palmolive R & D, Inc., Milmort, Belgium.
[§] Colgate-Palmolive Co., Piscataway, NJ.
[⊗] Abstract published in *Advance ACS Abstracts,* February 15, 1997.

(1) Yamanaka, T. *Bull. Chem. Soc. Jpn.* **1975**, *48*, 1755.
(2) Yamanaka, T. *Bull. Chem. Soc. Jpn.* **1975**, *48*, 1760.
(3) Kolarov, T.; Scheludko, A.; Exerova, D. *Trans. Faraday, Soc.* **1968**, *64*, 2864.
(4) Rudnev, V. S.; Rovin, Yu. G. *Colloid Zh.* **1984**, *46*, 743.
(5) Ivanov, I. B.; Dimitrov, D. S. In *Thin Liquid Films*; Ivanov, I. B., Ed.; Marcel Dekker: New York, 1988; p 379.
(6) Traykov, T. T.; Radoev, B. P.; Ivanov, I. B. *Ann. Univ. Sofia Fac. Chem.* **1970/1971**, *65*, 422.
(7) Dimitrov, D. S. *Biophys. J.* **1981**, *36*, 21.
(8) Dimitrov, D. S. *Prog. Surf. Sci.* **1983**, *14*, 295.

S0743-7463(96)00801-3 CCC: $14.00

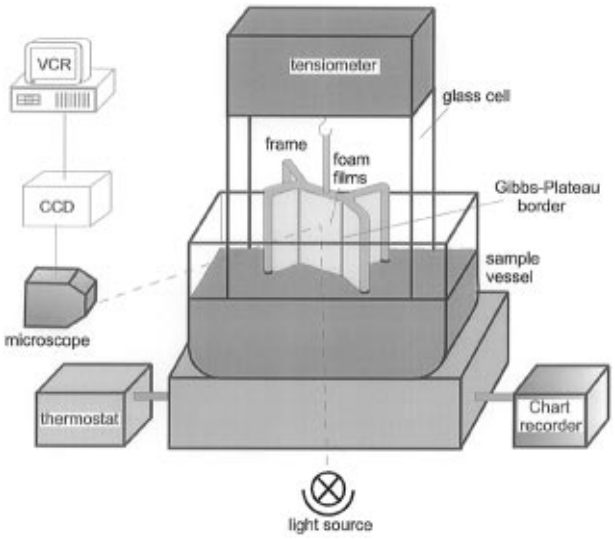

Figure 1. Scheme of the experimental setup for investigation of the drainage of vertical foam films.

foam film as well as to interpret quantitatively the experimental data for the additional tension, $\Delta\gamma$, vs the front velocity, v, at different electrolyte concentrations. We will mention in advance that our model shows how the driving force of the thin film expansion (the attractive disjoining pressure, Π) is related to the velocity of the front and the black film thickness. We demonstrate that in some cases steady capillary waves in the transition region can appear. The latter are gradually damped by the surface forces to ensure smooth profile of the thin film. In fact, the main dissipation of energy in the transition zone is concentrated into the region of capillary waves.

This work is organized as follows. In section 2 the experimental setup for vertical film formation and the procedure of measurement is described. Section 3 presents a mathematical model of the draining foam film. In section 4 we give some numerical results and compare the theory with the experimental data. The results and conclusions are summarized in section 5.

2. Experiment

Experimental Setup. The vertical macroscopic films were formed in a glass frame. In the literature there are several experimental methods described, for investigation of vertical liquid films.[9−11] The method we used is a modification of that of Lyklema[10] and Baets and Stein.[12] The experimental setup is depicted in Figure 1. It consists of a thermostatic table, sample vessel, mechanism for hanging the frame, which is connected with a tensiometer, and glass cell ensuring the space around the frame to be closed and saturated in order to avoid evaporation from the film. The solution was placed into a beaker on the table. The glass frames we used were with four sharp-angled legs (Figure 1) which form four foam films with a fifth film in the middle. The latter is situated between two vertical Gibbs−Plateau borders without direct contact with the frame. These five films drain simultaneously. It was convenient to measure the velocity of the film in the middle. The films were formed by moving the thermostatic table downward, observed by means of a horizontal microscope and recorded by a CCD camera and video system. The shape of the frame provides a better accuracy of the measurements of $\Delta\gamma$. The thickness was measured interferometrically[13] and the additional tension was measured by means of a Kruss K10ST tensiometer.

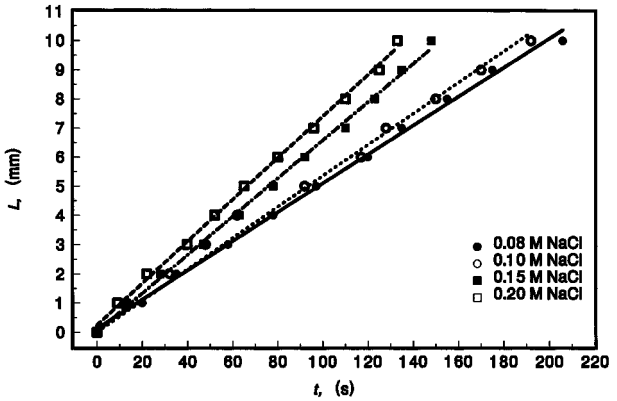

Figure 2. The total width, L, of the black film stripe vs time t at various NaCl concentrations. The films are stabilized by 0.05 wt % SDS.

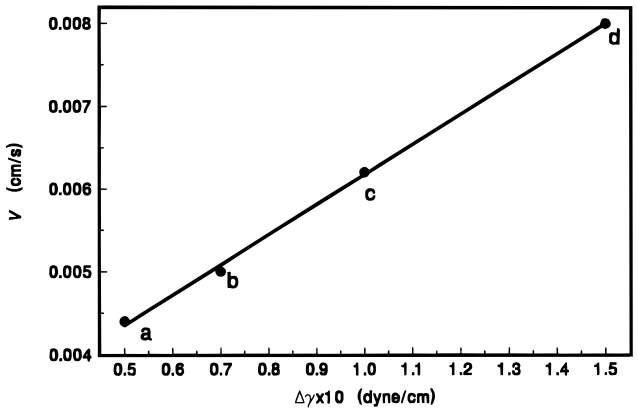

Figure 3. Front rate, v, vs the additional tension, $\Delta\gamma$ for various concentrations of NaCl: (a) 0.08 M; (b) 0.1 M; (c) 0.15 M; (d) 0.2 M. The films are stabilized by 0.05 wt % SDS.

All the experiments were carried out at constant temperature equal to 25 °C.

Materials. We studied films formed from solutions of sodium dodecyl sulfate (SDS) from Sigma without further purification at concentration 0.05 wt % and various ionic strengths adjusted by addition of NaCl from Merck. The concentration range of sodium chloride was between 0.08 and 0.2 M. Depending on the electrolyte concentration 0.08−0.2 M, the concentration of SDS is estimated to be 15−20 critical micelle concentration (cmc). At these conditions any impurities from dodecanol (if present) in SDS are believed to be solubilized and the solution surface tension is not influenced by them. All the solutions were prepared with deionized distilled water from a Millipore Milli Q System.

Experimental Results. The film formation is followed by spontaneous appearance and growth of a stripe of thin black film. Figure 2 shows the influence of the electrolyte concentration on the advance of the front between thin and thick films formed from 0.05 wt % SDS solutions containing different amounts of NaCl. The total height of the films in all of our experiments was constant and equal to 1.0 cm. It should be noted that the advancing front was *straight* and *horizontal* during its motion. In all cases the plots are straight lines (i.e., the black stripe grows with constant velocity), except in the final stage when it closely approaches the boundary with the bottom meniscus.

The dependence of the measured additional tension, $\Delta\gamma$, on the front rate, $v = dL/dt$, is plotted in Figure 3. The different points correspond to different concentrations of NaCl: 0.08, 0.1, 0.15, and 0.2 M. One sees the proportionality between the rate of front advance and the additional tension for this system (SDS and NaCl); moreover, the magnitude of the additional tension depends on the concentration of added electrolyte. For all these

(9) Hudales, J. B.; Stein, H. N. *J. Colloid Interface Sci.* **1990**, *138*, 354.
(10) Lyklema, J.; Scholten, P. C.; Mysels, K. J. *J. Phys. Chem.* **1965**, *69*, 116.
(11) Mysels, K. J.; Shinoda, K.; Frankel, S. *Soap Films, Studies of Their Thinning and a Bibliography*; Pergamon Press: New York, 1959.
(12) Baets, P. J. M.; Stein, H. N. *Langmuir* **1992**, *8*, 3099.
(13) Vasicek, A. *Optics of Thin Films*; North-Holland Publishing Co.: Amsterdam, 1960.

Table 1. Comparison between Theory and Experimental Data for the Additional Film Tension, $\Delta\gamma$, the Black Film Thickness, h, and Rate of Front Motion, v

C_{el}, (mol/l)	$v \times 10^3$ (cm/s)	$\Delta\gamma_{exper}$ (mN/m)	$\Delta\gamma_{theory}$ (mN/m)	$h_w^{experiment}$ (nm)	h_w^{theory} (nm)	A (nm^2)	$A_H \times 10^{19}$ (J)
0.08	0.0042	0.05	0.05	12.0	11.9	1.50	5.5
0.10	0.0050	0.07	0.06	11.0	10.8	1.60	4.9
0.15	0.0060	0.10	0.11	10.0	9.6	1.65	5.0
0.20	0.0080	0.15	0.17	8.0	8.0	1.60	5.3

films the final equilibrium thickness of the black film was measured, as well. The results obtained are summarized in Table 1, where data for the equilibrium thickness of the black film as a function of the NaCl concentration are also presented (see the end of section 4).

In order to check the possible effect of liquid drainage from the film into the marginal Gibbs−Plateau borders, we repeated the experiments with two simple rectangular glass frames (1 and 2 cm wide). The measured velocity of the front was found to be independent on the frame width and very close to that with the four-leg frame, originally used (Figure 1). Hence, the liquid drainage into the marginal channels practically does not affect the rate of front advance.

3. Hydrodynamic Model of the Front Motion

3.1. Physical Background. As seen in Figure 2 the rate of front advance (the slope of the curve) is *constant*, which means that the system has reached *stationary state*. In addition, Figure 3 shows the proportionality between the stationary front rate, v, and the jump of the film tension, $\Delta\gamma$, measured at the moment when the front between the black and the thicker film reaches the bottom meniscus,

$$\Delta\gamma = k_f v$$

If $\Delta\gamma$ can be interpreted as the driving force of the front motion, then k_f will have the meaning of coefficient of viscous friction. It has been shown experimentally by Yamanaka,[1] that k_f is proportional to the bulk viscosity of the solution. Thus, one can expect that the rate of front advance is determined by the bulk viscous friction in the thick film which counterbalances the driving force. The intuitive hypothesis that the driving force of the front motion downward is the weight of the thick film must be removed from the very beginning in so far as the rate of front motion is constant (independent from the film weight). As demonstrated below, the latter fact can be explained if the driving force of the process is identified with $\Delta\gamma$.

3.2. Mathematical Formulation of the Problem. Let us consider the section of a vertical foam film in the presence of front between the thick (I) and the thin (III) film−see Figure 4. We choose the coordinate plane Oxz to coincide with the film midplane. Then the profile of the film is defined by the equation

$$y = h(x,t) \tag{1}$$

where the x-axis is directed downward (see Figure 4) and t is time.

We will use the Navier−Stokes equation of the lubrication approximation (see, e.g., ref 14)

$$\frac{\partial p}{\partial x} - \rho g = \eta\frac{\partial^2 v_x}{\partial y^2}, \qquad \frac{\partial p}{\partial y} = 0 \tag{2}$$

which holds with a good accuracy for small interfacial slope ($dh/dx \ll 1$). Here p is the pressure in the film, v_x and v_y are the respective velocity components, and η is the dynamic viscosity.

(14) Landau, L. D.; Lifshitz, E. M. *Fluid Mechanics*; Pergamon Press: Oxford, 1980.

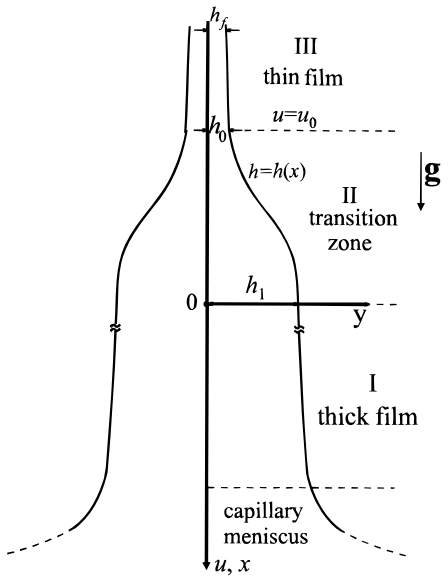

Figure 4. Sketch of the profile of a vertical draining foam film. The transition zone (ii) separates the regions of the thick film (I), where there is no disjoining pressure, $\Pi = 0$, and the thin film (II), where $\Pi \neq 0$.

The continuity equation reads

$$\frac{\partial v_x}{\partial x} + \frac{\partial v_y}{\partial y} = 0 \tag{3}$$

The kinematic boundary conditions at the film midplane follow from the symmetry of the problem

$$v_y|_{y=0} = 0 \qquad \text{and} \qquad \left.\frac{\partial v_x}{\partial y}\right|_{y=0} = 0 \tag{4}$$

We assume the film surfaces to be *tangentially immobile* due to presence of a large amount of surfactant in the solution. Usually, this condition is fulfilled with surfactants like sodium dodecyl sulfate (SDS) at comparatively high concentrations.[5] Then the kinematics boundary conditions at the film surfaces are

$$v_x^s = 0 \qquad \text{and} \qquad v_y^s = \frac{\partial h}{\partial t} \tag{5}$$

where the superscript "s" denotes the values of the velocity components at the film surface.

The final result from the integration of eqs 2 and 3 along with the boundary conditions eqs 4 and 5 reads

$$v_x = \frac{Q}{2\eta}(y^2 - h^2), \qquad v_y = \frac{y}{2\eta}\left[\frac{\partial}{\partial x}(h^2 Q) - \frac{y^2}{3}\frac{\partial Q}{\partial x}\right] \tag{6}$$

where we have introduced the auxiliary function

$$Q(x,t) \equiv \frac{\partial p}{\partial x} - \rho g \tag{7}$$

Then, the velocity component, v_y, at the film surface can be written in the form

$$v_y^s = v_y|_{y=h} = \frac{1}{3\eta}\frac{\partial}{\partial x}(h^3 Q) \tag{8}$$

which combined with eq 5 gives the equation governing the film profile

$$\frac{\partial h}{\partial t} = \frac{1}{3\eta}\frac{\partial}{\partial x}(h^3 Q) \tag{9}$$

An explicit expression for $Q(x,t)$ can be obtained by using the normal stress balance at the film surface

$$p = p_g - \sigma\frac{\partial^2 h}{\partial x^2} - \Pi(2h) \tag{10}$$

with σ and $\Pi(2h)$ being the film surface tension and the disjoining pressure isotherm. p_g is the pressure in the gaseous phase.

For the sake of convenience, we split the film into three parts: (I) thick foam film, (II) transition zone, and (III) thin liquid film of approximately constant thickness (see Figure 4). We will consider each of them separately, imposing appropriate boundary conditions.

3.3. The Thick Film (Region I). Let us consider the drainage of the thick foam film accompanying the motion of the front. We suppose that far above the liquid level the film is thinning steadily at constant liquid flux. On the other hand, near the horizontal liquid surface the film profile is very close to the shape of the respective static meniscus. Our aim here is to match the profile of the thick foam film with the capillary meniscus at the bottom of the film. For that purpose, we shall use an approach similar to that of Landau and Levich.[15,16] Since the thick film transforms into the capillary meniscus, one can expect that $h \to \infty$ and $dh/dx \to \infty$ for $x \to \infty$. However, the meniscus curvature (d^2h/dx for $x \to \infty$) is finite. Then following the procedure of Landau−Levich,[15] we require the curvature of the thick film, $h''(x)$, to approach the curvature of the capillary meniscus for $x \to \infty$. The meniscus shape is described by the Laplace equation of capillarity[14]

$$\frac{d^2H}{ds^2}\left[1 + \left(\frac{dH}{ds}\right)^2\right]^{-3/2} = \frac{\rho g}{\sigma}s \tag{11}$$

where the coordinate s increases as opposite of x and $s = 0$ at the level of the flat liquid surface (see Figure 5).

Since the thick film is approximately plane-parallel far from the liquid level, the matching can be performed at the point where $dH/ds = 0$. From the first integral of eq 11 we find that $dH/ds = 0$ at $s^* = (2\sigma/\rho g)^{1/2}$. Actually, s^* has the meaning of the capillary rise of liquid at a completely wettable wall. The substitution of $s = s^*$ into eq 11 gives the required value of the second derivative

$$\left.\frac{d^2H}{ds^2}\right|_{s^*} = \left(\frac{2\rho g}{\sigma}\right)^{1/2} \tag{12}$$

Thus the conditions for matching of the capillary meniscus with the thick film read

$$H \to 0, \quad dH/ds \to 0, \quad d^2H/ds^2 \to (2\rho g/\sigma)^{1/2} \quad \text{at} \quad s \to s^* \tag{13}$$

Let us proceed with the thick film (I) profile. We assume a steady profile of the thick foam film

$$\partial h/\partial t = 0 \tag{14}$$

which combined with eqs 9 and 10 gives

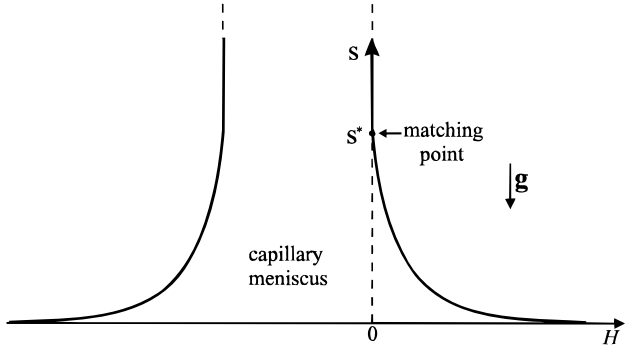

Figure 5. Sketch of the capillary meniscus at the bottom of the film.

$$h^3\left(\sigma\frac{d^3h}{dx^3} + \rho g\right) = 3\eta j_1 \tag{15}$$

Here the integration has been carried out along with a boundary condition for constant liquid flux

$$j|_{x=0} = j_1, \qquad h|_{x=0} = h_1 \tag{16}$$

at the point $x = 0$. In fact, this point can be considered as a fictive boundary between the thick film (I) and the transition zone (II)−see Figure 4.

In terms of the dimensionless variables

$$f = h/h_1, \qquad \xi = \lambda x, \qquad \beta = [\rho g/(\sigma h_1 \lambda^2)], \qquad \lambda = (3\eta j_1/\sigma h_1^4)^{1/3} \tag{17}$$

eq 15 acquires the form

$$\frac{d^3f}{d\xi^3} + \beta = \frac{1}{f^3} \tag{18}$$

One can estimate that for the typical values of the parameters: $h_1 \sim 1\ \mu$m, $\sigma = 30$ mN/m, $\rho = 1$ g/cm^3, $j_1 \approx h_1 v \sim 10^{-5}$ cm^2/s, $\lambda^{-1} \sim 22\ \mu$m, the parameter $\beta \approx 3 \times 10^{-7}$ is a very small quantity and can be neglected without a loss of accuracy. The latter estimate is consonant with the Levich[16] conclusion that the vertical film drainage (for thick film) is governed by the capillary suction of the meniscus rather than by gravity. The omission of β in eq 18 simplifies the problem considerably, because the equation obtained

$$\frac{d^3f}{d\xi^3} = \frac{1}{f^3} \tag{18a}$$

does not contain any physical parameters and can be solved numerically with the following initial conditions

$$f(0) = 1, \qquad f'(0) = 0, \qquad f''(0) = 0 \tag{19}$$

The physical meaning of eqs 19 is that the thick foam film becomes flat *asymptotically* far away from the capillary meniscus. Note that the initial conditions, eqs 19, are also free of physical parameters. On the other hand, one sees from eq 18a that the third derivative of the solution $f'''(\xi)$ vanishes when $\xi \to \infty$ since $f \to \infty$. Hence the profile second derivative should approach constant at $\epsilon \to \infty$, which we determine by numerically solving eq 18a

$$f''(\xi \to \infty) \to k_s = 1.2650 \tag{20}$$

Actually, eq 20 gives the value of the dimensionless curvature of the film profile when it approaches the

(15) Landau L. D.; Levich, V. G. *Acta Phys. Chem. USSR* **1945**, *20*, 6.

(16) Levich, V. G. *Physicochemical Hydrodynamics*; Prentice-Hall: Englewood Cliffs, NJ, 1962.

capillary meniscus. Then the matching condition requires the equality of the curvature of the static meniscus when $H \to 0$ ($s \to s^*$) with the curvature of the film at large thickness, (at $x \to \infty$)

$$\left(\frac{d^2H}{ds^2}\right)_{s\to s^*}^{\text{meniscus}} = \left(\frac{d^2h}{dx^2}\right)_{x\to\infty}^{\text{film}} \quad (21)$$

Using eqs 11−13, 15−17, and 21, we find the following relationship between the liquid flux, j_1, and the thickness h_1 of the thick film (I)

$$j_1 = \frac{\sigma^{1/4}(2\rho g)^{3/4}h_1^{5/2}}{3\eta k_s^{3/2}} \quad (22)$$

On the other hand, the liquid flux j_1 at $x = 0$ has to be determined from the matching with the profile of the transition zone, close to the thin black film—see below.

3.4. The Transition Zone (Region II). The equation governing the film profile in the transition zone (II) can be obtained by the following analysis. We are seeking for a solution of eq 9 in the form of propagating wave

$$h(x,t) \equiv h(x - vt) = h(u), \qquad u \equiv x - vt \quad (23)$$

which corresponds to a simple translation of the film profile along the x-axis with velocity v. The later is possible because eq 9 does not contain the coordinate x and the time t, explicitly. Substituting eq 23 into eq 9 and performing the integration we get

$$-3\eta v h(u) = h(u)^3 Q(u) + C \quad (24)$$

The integration constant, C, is to be determined from the condition for zero flux at $h = h_0$

$$Q(u) = \frac{dp}{du} - \rho g = 0 \quad \text{at} \quad h = h_0 \quad (25)$$

since the thin liquid film (III) is considered to be in rest (cf. Figure 4). Actually, h_0 does not coincide with the thickness of the thin liquid film (III). The point $h = h_0$ is a fictive boundary between the transition zone (II) and the thin black film (III) where the liquid flux vanishes.

After the substitution of the normal stress balance, eq 10, into eq 24 and using eq 25 we obtain

$$\frac{3\eta v(h - h_0)}{h^3} = \sigma\frac{d^3h}{du^3} + 2\Pi'(2h)\frac{dh}{du} + \rho g \quad (26)$$

Equation 26 describes the profile of the transition zone (II) between the thick foam film (I) and the thin black film (III).

On the other hand, it follows from eqs 9, 15, and 23 that the liquid flux at the point $x = 0$ has the form

$$j_1 = v(h_1 - h_0) \approx vh_1, \qquad h_0/h_1 \ll 1 \quad (27)$$

Combining eqs 22 and 27 we express the thickness of the thick foam film (I) at $x = 0$

$$h_1 \approx \frac{k_s(3\eta v)^{2/3}}{\sigma^{1/6}(2\rho g)^{1/2}} \quad (28)$$

For the typical values of $\sigma = 30$ mN/m, $\rho = 1$ g/cm^3, and $\eta = 0.01$ P and for velocities v $= 10^{-3}$−10^{-2} cm/s we estimate that $h_1 = 0.16$−$0.73\,\mu$m. If we introduce similar dimensionless variables as in eq 17, viz.

$$f = h/h_1, \qquad \epsilon = h_0/h_1, \qquad \xi = \lambda u,$$
$$\lambda = (3\eta v/\sigma)^{1/3}/h_1, \qquad \delta = [\rho g/(\sigma h_1\lambda^2)] \quad (29)$$

eq 26 can be transformed to read

$$\frac{d^3f}{d\xi^3} - \alpha(f)\frac{df}{d\xi} + \delta = \frac{(f - \epsilon)}{f^3} \quad (30)$$

where the coefficient function, $\alpha(f)$, is defined as follows

$$\alpha(f) \equiv -\frac{2\Pi'(2h_1f)}{\sigma\lambda^2} \quad (31)$$

Estimation, similar to this after eq 18, shows that the parameter δ, explicitly containing the gravity effects, can be neglected without a loss of accuracy. The resulting equation,

$$\frac{d^3f}{d\xi^3} - \alpha(f)\frac{df}{d\xi} = \frac{(f - \epsilon)}{f^3} \quad (32)$$

which should be integrated backward, starting from the point $\xi = 0$ ($x = 0$) with the same initial conditions as eqs 19. However, the value $h(u_0) = h_0$ at the end point (where $f(\epsilon_0) = \epsilon$) is not a priori known. We shall determine it from the condition for matching of the solution of eq 32 with the thin black film (III)—see below.

3.5. The Thin Black Film (Region III). We assume that the *thin black film* (III) above the transition zone (Figure 4) is approximately flat. The latter is fulfilled with high accuracy since the disjoining pressure isotherm is very steep and the variations of the film thickness due to gravity effects are negligible (smaller than the experimental error of the film thickness measurements).

The profile of the thin liquid film is determined from the condition for equilibrium

$$\frac{dp}{du} - \rho g = 0 \quad (33)$$

which combined with the normal stress balance, eq 10 and eq 29, yields

$$\frac{d^3f}{d\xi^3} - \alpha(f)\frac{df}{d\xi} = -\delta \quad (34)$$

Since the thin liquid film is approximately flat, one can linearize eq 34 for small deviations, $\zeta(\xi)$, from constant c_0

$$f(\xi) = c_0 + \zeta(\xi), \qquad |\zeta(\xi)| \ll c_0 \quad (35)$$

$$\frac{d^3\zeta}{d\xi^3} - \alpha_0\frac{d\zeta}{d\xi} = -\delta, \qquad \alpha_0 = \alpha(\epsilon) \quad (36)$$

where the typical values of the coefficients are $\alpha_0 \sim 10$−1000, $\delta \sim 10^{-5}$−10^{-7}. One sees that the parameter δ can be neglected in eqs 34−36. The characteristic polynomial of eq 36 reads

$$r^3 - \alpha_0 r = 0 \quad (37)$$

which roots (r_k, $k = 1, 2, 3$) determine its eigenvalues. Then the respective solution of eq 34 can be written in the form

$$f(\xi) \approx c_0 + c_1 \exp((\xi - \xi_0)\sqrt{\alpha_0}) + c_2 \exp(-(\xi - \xi_0)\sqrt{\alpha_0}) \quad (38)$$

$$\xi \le \xi_0$$

where the integration constants c_0, c_1, and c_2 are to be determined from the matching of eq 38 with the profile of the transition zone. From the solution and its derivatives in the matching point, $\xi = \xi_0$

$$f_0 = f(\xi_0) = \epsilon, \qquad f_0' = f'(\xi_0), \qquad f_0'' = f''(\xi_0) \quad (39)$$

we can express the integration constants in eq 38 in the form

$$c_0 = 1 - \frac{f_0''}{\alpha_0}, \qquad c_1 = \frac{f_0'' + f_0'\sqrt{\alpha_0}}{2\alpha_0}, \qquad c_2 = \frac{f_0'' - f_0'\sqrt{\alpha_0}}{2\alpha_0} \quad (40)$$

On the other hand, we require the thin film profile to level off constant when $\xi \to -\infty$. The latter is equivalent to the requirement to vanish the coefficient at the growing exponent in eq 38, i.e., $c_2 = 0$. One sees from eq 40 that in the matching point, $\xi = \xi_0$, the following relationship between the solution derivatives should be satisfied

$$f''(\xi_0) = f'(\xi_0)\sqrt{\alpha_0} \quad (41)$$

Equation 41 gives the criteria for determining the fictive boundary between the transition zone (II) and the black film (III).

Let us come back to the integration of eq 32, describing the profile of the transition zone. In order to ensure a smooth matching (up to second derivative) of the transition zone with the thin film, we adopted the following procedure. We choose a trial value for h_0 when calculating the coefficient function, $\alpha(f)$, and then we integrate eq 32 backward starting from $\xi = 0$ with the initial conditions, eqs 19, until the solution equals ϵ, $f(\xi_0) = \epsilon$, (or $h(u_0) = h_0$) which determines the end point, $\xi = \xi_0$. We vary the value of h_0 until the relationship, eq 41, is satisfied. The thin film profile can be continued smoothly from the matching point, $\xi = \xi_0$, according to the equation

$$f(\xi) \approx \epsilon - \frac{f_0''}{\alpha_0}[1 - \exp((\xi - \xi_0)\sqrt{\alpha_0})] \quad (42)$$

$$\xi < \xi_0$$

where only the decaying exponent at $\xi \to -\infty$ is left from eq 38. One sees that the final dimensionless thickness of the thin film is less than unity (i.e., $h < h_0$ for $u < u_0$). In dimensional units we calculate the thickness, h_f, of the black film

$$h_f = h(u \to -\infty) = h_0 + \frac{\sigma h_0''}{2\Pi'(2h_0)} \quad (43)$$

which is an experimentally measurable quantity. Note that the disjoining pressure derivative is negative at $h = h_0$.

3.6. Driving Force of the Front Motion. Since the film drainage is supposed to reach steady state, the driving force of the process is mutually counterbalanced by the viscous friction in the film. Then we can determine the driving force by integrating the viscous stress, τ_{xy}, along the transition zone up to the capillary meniscus

$$\Delta\gamma = -2\int_{u \ge u_0} \tau_{xy}|_{y=h}\, du = -2\int_{u \ge u_0} \eta \left.\frac{\partial v_x}{\partial y}\right|_{y=h} du \quad (44)$$

After the substitution of eq 6 into eq 44, we can split the integral in two parts:

$$\Delta\gamma = \Delta\gamma_0 + \Delta\gamma_1 \quad (45)$$

where

$$\Delta\gamma_0 = -2\int_{u_0}^{0} Q(u)h(u)\, du \quad (46)$$

is the contribution of the transition zone (II) and

$$\Delta\gamma_1 = -2\int_0^\infty Q(x)h(x)\, dx \quad (47)$$

is that of the thick foam film (I). Using eqs 7, 10, 19, and 32 we calculate

$$\Delta\gamma_0 \approx \sigma(h_0'^2 - 2h_0h_0'') - 2h_0\Pi(2h_0) - \int_{2h_0}^\infty \Pi(x)\, dx \quad (48)$$

where $h_0' = h'(u_0)$ and $h_0'' = h''(u_0)$. On the other hand, using eqs 17, 18a and 47 we obtain the following estimate for $\Delta\gamma_1$:

$$\Delta\gamma_1 \approx \frac{6\eta j_1}{\lambda h_1^2} I, \qquad I = \int_0^\infty \frac{d\xi}{f(\xi)^2} \quad (49)$$

The integral I can be calculated from the numerical solution of eq 18a with the initial conditions, eqs 19, to give $I \approx 1.539$ and

$$\Delta\gamma_1 \approx 2(3\eta v)^{2/3} I \approx 6.44(\eta v)^{2/3} \quad (50)$$

One sees that for $\eta = 10^{-2}$ P and $v \sim 10^{-3}$ cm/s, $\Delta\gamma_1 \sim 10^{-3}$ mN/m which is one order of magnitude less than the values of $\Delta\gamma$ measured in the experiment—see Figure 3 and Table 1. Hence, the main contribution to $\Delta\gamma$ is expected to come from the transition zone, $\Delta\gamma \approx \Delta\gamma_0$, as demonstrated below.

4. Numerical Results and Comparison with the Experiment

Our aim is to interpret the experimental data for drainage of vertical foam film formed from solutions of sodium dodecyl sulfate (SDS) and NaCl. With this end in view we use the disjoining pressure isotherm of the conventional DLVO theory[17]

$$\Pi(H) = \Pi_{el}(H) + \Pi_{vw}(H) \quad (51)$$

where

$$\Pi_{vw}(H) = -\frac{A_H}{6\pi h_w^3}, \qquad h_w \approx H + 2h_{tails} \quad (52)$$

is the van der Waals disjoining pressure with h_w being the so-called "equivalent water thickness" that contains the both the film water core of thickness, H, and the two surfactant monolayers. In our calculations we use $h_{tails} = 1$ nm. The electrostatic disjoining pressure we calculate at *constant surface charge*, σ_s

(17) Verwey, E. J. W.; Overbeek, J. Th. G. *Theory of the Stability of Lyophobic Colloids*; Elsevier: Amsterdam, 1948; p 5.

$$\Pi_{el}(H) = \frac{8\pi\sigma_s^2}{\epsilon}\frac{\exp(-\kappa H)}{1-\exp(-\kappa H)}, \qquad \sigma_s^2 = \frac{e^2}{A^2} = \text{const} \tag{53}$$

Here e is the electron charge, A is the area per surface charge, $\epsilon = 80$ is the water dielectric permittivity,

$$\kappa = [8\pi e^2 n_0/\epsilon kT]^{1/2} \tag{54}$$

is the reverse Debye length with n_0 being the electrolyte concentration.

Our aim here is to compare the outcome of the theory with the experimentally determined additional tension, $\Delta\gamma$, and the rate of front motion, v, at various electrolyte concentrations. We use the Hamaker constant, A_H, and the area per surface charge, A, as adjustable parameters when calculating the foam film profile and the respective value of the additional tension. The computational procedure we use is the following. For a given concentration of electrolyte, C_{el}, and the measured front motion rate, v, we choose some values of A_H and A. Then the profile of the transition zone is calculated by numerical integration of eq 32 with the initial conditions, eqs 19. The values of h_0 and h_f are determined according to the procedure described in section 3 (cf. eqs 41 and 43). Finally, the calculation of the additional tension is done according to eqs 45, 48, and 50.

In Table 1 the experimental data were interpreted with our theoretical model. One can see that the theory agrees well with the data for the measured driving forces at the cost of very large values of the Hamaker constant, A_H, that are about 1 order of magnitude larger than that predicted by the Lifshitz theory[18] (usually $A_H \sim 3.7 \times 10^{-20}$ J for foam films—see, e.g., ref 19). The reason is that the electrolyte concentration is too high and the DLVO theory is not valid under these conditions. This means that the larger Hamaker constant incorporates the effect of ionic correlation surface force that is operative at these electrolyte concentrations. Besides, the effects due to ionic exclusion volume and discreteness of the surface charge should also be accounted for in this case. In other words, the calculated values of the parameters in the disjoining pressure isotherm, eqs 51−53, do not have the exact physical meaning, accepted in the conventional DLVO theory, irrespective of the good fit of the experimental data.[20] For the time being there is no quantitative theory of the surface forces at high electrolyte concentrations like these in our experiments. That is why the DLVO $\Pi(H)$ isotherm can only be used as a semiempirical curve for fitting the surface force with adjustable parameters. The fact that the calculated values of A and A_H (Table 1) are practically the same for all electrolyte concentrations favors the usage of this semiempirical $\Pi(H)$ isotherm, which accounts adequately at least for the effect of electrolyte.

Our theory of the front motion also agrees qualitatively with the experimental data of Yamanaka,[1] but unfortunately, in the latter study the thickness of the black films formed are not presented, and it is not possible to make a quantitative comparison.

Figure 6a illustrates the profile of the transition zone computed by numerical integration of eq 32. The point $\xi = 0$ represents the matching point with the thick foam film whose profile is not shown in the figure. Note that

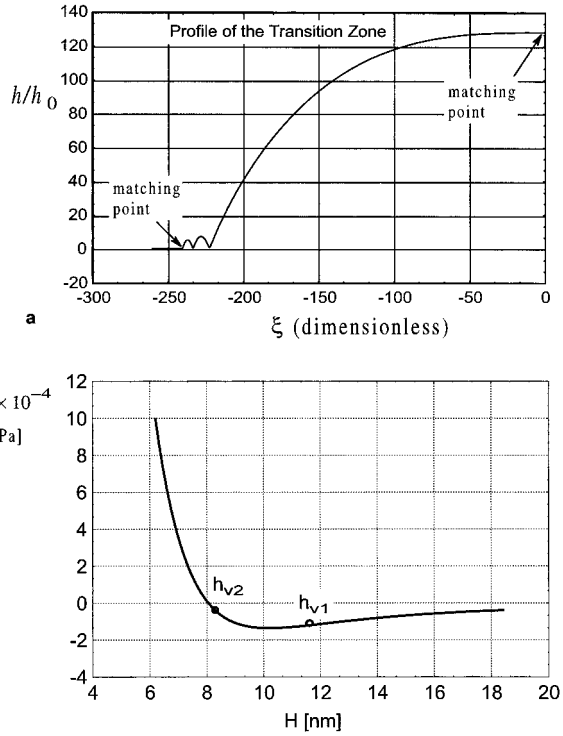

Figure 6. (a) The computed profile of the transition zone of the draining foam film, h/h_0 vs ξ. The values of the parameters are $\sigma = 32.3$ mN/m, $C_{el} = 0.2$ M, $v = 80$ μm/s, $A_H = 5.3 \times 10^{-19}$ J, and $A = 1.6$ nm^2. (b) The disjoining pressure isotherm $\Pi(H) = \Pi_{vw}(H) + \Pi_{el}(H)$ used in the calculations. The points $H = h_{v1}$ and $H = h_{v2}$ lie on the right and the left branches of the curve $\Pi(H)$, respectively.

the film profile is flat near this point but considerably varies in the transition zone. One sees that the presence of oscillatory profile the waves in the beginning of the transition zone where it matches with the profile of the thin liquid film (the flat part). These steady capillary waves are a result of the combined action of the capillary pressure, viscous friction, and disjoining pressure.

The origin of the steady capillary waves can be understood by means of the following analysis. Let us take some point of thickness h_{v_1} in the right branch of the disjoining pressure isotherm (see Figure 6b), where the van der Waals forces are dominant. For the sake of estimation we linearize eq 32 for small deviations of the profile around this thickness, $h = h_{v1} + \zeta$. The resulting equation reads

$$\zeta''' + b\zeta' - \zeta = 0, \qquad b = \text{const} \tag{55}$$

The characteristic polynomial of this equation

$$r^3 + br - 1 = 0 \tag{56}$$

has always one real positive and two complex roots of negative real parts for positive b. When b approaches zero (at the minimum of the disjoining pressure isotherm) the roots are $r_1 = 1$, $r_{2,3} = -1/2 \pm i\sqrt{3/2}$. One sees that even without surface forces an oscillatory profile of the film can be obtained and the attractive van der Waals forces just modify the wave period and amplitude. Similar wavelike film profiles have also been calculated by Churaev[21] in the case of advancing meniscus in very thin capillaries. One can also make an analogy with the classical work of Kapitza, 1948 (see, e.g., ref 16) where traveling capillary waves at the surface of vertical wetting

(18) Lifshitz, E. M. *Sov. Phys. JETP (Engl. Transl.)* **1956**, *2*, 73.
(19) Israelashvili, J. *Intermolecular & Surface Forces*; Academic Press: London, 1992.
(20) Overbeek, J. Th. G. In *Colloid Science*; Kruyt, H. R., Ed.; Elsevier: Amsterdam, 1952; Vol. 1, Chapter 3.
(21) Churaev, N. V. *Rev. Phys. Appl.* **1988**, 975.

film have been investigated theoretically. However, in this case the steady dissipation of energy is due to the exact balance of the work done by gravity with the viscous dissipation of energy in the capillary waves, while in our case the steady oscillatory profile is due to the balance of the work done by the surface forces (the disjoining pressure) with viscous dissipation of energy in the transition zone.

On the other hand, if the point h_{v2} is on the left branch of the disjoining pressure isotherm, where the repulsive electrostatic disjoining pressure is also operative, $b < 0$, and the solution of eq 55 has qualitatively different behavior. Then eq 56 can also have one real positive and two complex roots of negative real parts, but only if the isotherm slope, $d\Pi/dh$, is smaller than some critical value ($|b| < 1.89$). Otherwise, if the slope is larger ($|b| > 1.89$) there are three real roots of eq 56 (one positive and two negative) and the profile is monotonic.

5. Concluding Remarks

We have determined experimentally the rate of motion of the front between thin and thick film into a macroscopic vertical foam film as a function of the electrolyte concentration. The experiment gives also the additional tension and the thin (black) film thickness. The used frame with four sharp-edged legs allows us to measure the additional tension more accurately compared to the simplest rectangular frame.[1] The rate of the front motion is constant and is proportional to the additional tension, as previously obtained by Yamanaka.[1,2]

We have developed a hydrodynamic theory of the front motion which allows calculation of the driving force of the process and the black film thickness at a given front rate. The theory shows a good agreement with the experimental data.

The main findings of this study are the following:

(i) The driving force of the front motion is a superposition of attractive disjoining pressure and capillary pressure effects—see eq 48.

(ii) The energy dissipation during the film drainage is concentrated mainly in the transition zone between the black and thicker foam film; i.e., the viscous friction in the thick film can be neglected (cf. eq 50).

(iii) The computed profiles of the transition zone where the main energy dissipation happens showed the presence of steady capillary waves in the beginning of the transition zone as a result of combined action of capillary effects, viscous friction, and surface forces.

(iv) The disjoining pressure contributes to the driving force of the drainage and modifies and damps the steady capillary waves in the region of the black film.

We believe the above theoretical model can be modified to treat the case of expansion of circular spots in microscopic films where similar behavior has been observed.[3,4] The theory can be further extended to describe the motion of the series of stripes of different thickness in vertical stratifying films. Such studies are under way.

Acknowledgment. This study was supported financially by Colgate-Palmolive Inc., and in part, by the Bulgarian National Science Fund. Useful discussions with Professor Peter Kralchevsky and Dr. Krassimir Danov are greatly acknowledged.

LA9608019